Intermolecular transmission of superoxide dismutase 1 misfolding in living cells

Leslie I. Grad[a,1], Will C. Guest[a,1], Anat Yanai[a], Edward Pokrishevsky[a], Megan A. O'Neill[a], Ebrima Gibbs[a], Valentyna Semenchenko[b], Masoud Yousefi[a], David S. Wishart[c], Steven S. Plotkin[d], and Neil R. Cashman[a,2]

[a]Brain Research Centre, University of British Columbia, Vancouver, BC, Canada V6T 2B5; [b]National Institute for Nanotechnology, Edmonton, AB, Canada T6G 2M9; [c]Departments of Biological Sciences and Computing Science, University of Alberta, Edmonton, AB, Canada, T6G 2E8; and [d]Department of Physics and Astronomy, University of British Columbia, Vancouver, BC, Canada V6T 1Z1

Edited* by Don W. Cleveland, University of California at San Diego, La Jolla, CA, and approved July 25, 2011 (received for review February 23, 2011)

Human wild-type superoxide dismutase-1 (wtSOD1) is known to coaggregate with mutant SOD1 in familial amyotrophic lateral sclerosis (FALS), in double transgenic models of FALS, and in cell culture systems, but the structural determinants of this process are unclear. Here we molecularly dissect the effects of intracellular and cell-free obligately misfolded SOD1 mutant proteins on natively structured wild-type SOD1. Expression of the enzymatically inactive, natural familial ALS SOD1 mutations G127X and G85R in human mesenchymal and neural cell lines induces misfolding of wild-type natively structured SOD1, as indicated by: acquisition of immunoreactivity with SOD1 misfolding-specific monoclonal antibodies; markedly enhanced protease sensitivity suggestive of structural loosening; and nonnative disulfide-linked oligomer and multimer formation. Expression of G127X and G85R in mouse cell lines did not induce misfolding of murine wtSOD1, and a species restriction element for human wtSOD1 conversion was mapped to a region of sequence divergence in loop II and β-strand 3 of the SOD1 β-barrel (residues 24–36), then further refined surprisingly to a single tryptophan residue at codon 32 (W32) in human SOD1. Time course experiments enabled by W32 restriction revealed that G127X and misfolded wtSOD1 can induce misfolding of cell-endogenous wtSOD1. Finally, aggregated recombinant G127X is capable of inducing misfolding and protease sensitivity of recombinant human wtSOD1 in a cell-free system containing reducing and chelating agents; cell-free wtSOD1 conversion was also restricted by W32. These observations demonstrate that misfolded SOD1 can induce misfolding of natively structured wtSOD1 in a physiological intracellular milieu, consistent with a direct protein–protein interaction.

neurodegeneration | protein misfolding | prion | template-directed misfolding | seeded polymerization

Amyotrophic lateral sclerosis (ALS) is caused by the degeneration of motor neurons in the brain, brainstem, and spinal cord (1), resulting in progressive paralysis of the limbs and the muscles of speech, swallowing, and respiration. ALS is responsible for approximately 1 in 1,000 adult deaths, with 80% of individuals dying within 2–5 y of diagnosis (2). Approximately 10% of ALS cases display autosomal dominant inheritance (3), with ≈20% of these cases due to mutations in the gene encoding superoxide dismutase 1 (SOD1) (4), a ubiquitously expressed free radical defense enzyme abundantly expressed in motor neurons. More than 151 familial ALS (FALS) SOD1 missense, nonsense, and intron splice-disrupting mutations have been cataloged to date (5) (http://alsod.iop.kcl.ac.uk/), with no benign amino acid polymorphisms as yet identified. The collective evidence suggests that a cytotoxic gain of function is conferred by SOD1 mutations (1, 6), which has been variously attributed to generation of reactive oxygen and nitrogen species, cytoskeletal disruption, caspase activation, mitochondrial dysfunction, proteosome disruption, microglial activation, and other mechanisms (1, 7). A well-studied consequence of SOD1 mutation and/or oxidation is a propensity of the protein to misfold and aggregate (8). SOD1-containing neural deposits can be detected by immunohistochemistry (IHC) in motor neurons from familial ALS patients (9) and in transgenic (10) and tissue culture (11) models of the disease. Emerging evidence with misfolding-specific antibodies also identifies misfolded SOD1 in sporadic ALS (SALS) (12, 13), although some antibodies recognizing misfolded SOD1 in FALS do not show immunoreactivity in SALS (e.g., ref. 14).

Protein misfolding diseases have been classically understood as errors in proteostasis, in which the burden of misfolded species eventually overwhelms the compensatory mechanisms that normally keep their concentration low (8). Alternatively, a pathologically disordered protein may recruit and induce misfolding of a natively folded isoform, by seeded polymerization or template assistance (15). These molecular mechanisms may participate in the pathogenesis of several neurodegenerative conditions, including prion disease, Alzheimer's disease, and Parkinson's disease (16). However, detailed molecular mechanisms are lacking for the propagation of protein misfolding in these diseases.

ALS shows spatiotemporal propagation through the neuroaxis (17), consistent with propagated protein misfolding. Implication of SOD1 in this process is suggested by studies showing that misfolded SOD1 is efficiently exported and imported by cells (18, 19). In an intriguing recent study (20), aggregates of misfolded mutant SOD1 were shown to be taken up from the extracellular environment by macropinocytosis and cause misfolding of endogenously expressed mutant SOD1. Here we consider the intracellular consequences of obligate misfolded SOD1 mutants G127X and G85R on the structure of wild-type SOD1 (wtSOD1). We developed a constrained system in vitro in which cause and effect of participating SOD1 molecular species in misfolding can be effectively disentangled. We exploited two natural FALS SOD1 mutants: G127X, comprising a TGGG frameshift insertion in exon 5, and the full-length missense mutation G85R (Fig. 1 *A* and *B*). Both G127X and G85R translation products migrate faster than wtSOD1 on gel electrophoresis, which can be visualized by direct immunoblotting as probed with panspecific SOD1 affinity purified rabbit IgG. G127X possesses the added convenience of being distinguishable from wtSOD1 by mutually exclusive polyclonal antibodies (pAbs): one directed against the five nonnative amino acids following Gly127 in the G127X SOD1 variant (GX-CT), the other directed

Author contributions: L.I.G., W.C.G., A.Y., M.A.O., E.G., and N.R.C. designed research; L.I.G., W.C.G., A.Y., E.P., M.A.O., E.G., and N.R.C. performed research; V.S., D.S.W., and N.R.C. contributed new reagents/analytic tools; L.I.G., W.C.G., A.Y., E.P., M.A.O., E.G., M.Y., S.S.P., and N.R.C. analyzed data; and L.I.G., W.C.G., and N.R.C. wrote the paper.

Conflict of interest statement: Neil R. Cashman is co-founder and Chief Scientific Officer of Amorfix Life Sciences, a Canadian biotechnology company assigned intellectual property associated with the antibodies directed against disease-specific epitopes used in this study.

*This Direct Submission article had a prearranged editor.

[1]L.I.G. and W.C.G. contributed equally to this work.

[2]To whom correspondence should be addressed. E-mail: neil.cashman@vch.ca.

This article contains supporting information online at www.pnas.org/lookup/suppl/doi:10.1073/pnas.1102645108/-/DCSupplemental.

against the C-terminal 25 amino acids of wtSOD1 deleted in the G127X mutant (WT-CT) (Fig. 1 *A* and *B*). G127X expression also provides an opportunity to unambiguously identify induced misfolding of wtSOD1 by recognition of SOD1 misfolding-exposed epitopes in the deleted region, particularly by nondenaturing methods such as immunoprecipitation (IP) and immunofluorescence (IF) of "native" misfolded wtSOD1.

Results

Expression of Misfolded SOD1 Induces Misfolding of wtSOD1 in Human Cells. We selected two disease-specific epitopes (DSEs) of wtSOD1 (DSE1a and DSE2) (Fig. 1*A*), specifically recognizing regions inaccessible to antibody binding in natively structured wtSOD1 but exposed on the molecular surface of the misfolded isoforms (21, 22). DSE1a comprises residues 145–151 [the SOD1 epitope of the dimer interface, SEDI, previously reported (23)] with cysteic acid replacing Cys146. Substitution of this sulfonic acid derivative in SEDI was based on the reasoning that sulfhydryl Cys146, exposed by Cys57–Cys146 intrachain disulfide bond reduction accompanying dimer dissociation (24), is a ready substrate for oxidative modifications. 10C12, the DSE1a mAb used in these studies, specifically binds to in vitro oxidized SOD1 and disease-associated misfolded SOD1 as determined by ELISA, IP, and IHC (22). DSE2 comprises residues 125–142 that form a segment of the SOD1 electrostatic loop, a structural element that is extruded and interacting with β-barrel elements in crystal structures of aggregated SOD1 (25). 3H1, the DSE2 mAb used in these studies, specifically binds to SOD1 that has been misfolded in vitro by denaturants and mild oxidation, and to disease-associated misfolded SOD1 by IP, IF, and IHC (21, 22).

G127X and G85R SOD1 proteins are partially misfolded, enzymatically inactive SOD1 molecular species, which do not stoichiometrically bind structure-promoting copper or zinc ions (26, 27). Moreover, the Cys146 necessary for formation of the monomer-stabilizing intrachain disulfide bond is deleted in G127X. Relative to wtSOD1, the instability of G85R has been demonstrated by its considerably reduced unfolding temperature in calorimetric studies (28). Equivalent data are unavailable for G127X, but equilibrium molecular dynamics simulation showed greater regional structural fluctuation compared with wild-type protein (Fig. S1*A*).

For these studies, we used an experimentally tractable cell culture system that did not overexpress human wtSOD1 (associated with spontaneous misfolding in vitro and in vivo (29, 30)]. Transient transfection-mediated expression of G127X or G85R in HEK-293FT (HEK) cells induced misfolding of endogenously expressed human wtSOD1, as observed by IF microscopy with the DSE mAb 3H1 (Fig. 1 *C–F*) and by IP with the DSE mAbs 3H1 and 10C12 (Fig. 2*A*). To ensure that these observations are not merely due to stressors associated with the transfection process, all experiments include an empty vector (EV) control in which cells are transfected with noncoding DNA. G127X expression in HEK cells permitted the unambiguous colocalization of mutant and misfolded wtSOD1, showing coincident immunoreactivity for GX-CT and DSE2-3H1 in 21% of transfected cells (2,000 GX-CT$^+$ cells counted). Inspection of IF images show that within doubly positive cells immunoreactivity for G127X and misfolded wtSOD1 were not entirely congruent, and immunoreactivity for 3H1 had a punctate appearance, both of which may reflect differences in trafficking, consolidation, or degradation of the mutant and wild-type misfolded proteins. Because G85R SOD1 possesses the DSE epitopes, distinction of mutant and wtSOD1 misfolded species was not possible by IF. Molecular association of misfolded wtSOD1 with G127X was demonstrated by co-IP of mutant and misfolded wtSOD1 in nondenaturated HEK lysates from mutant-transfected HEK cells probed with GX-CT-, 10C12- or 3H1-coupled magnetic beads and detected on subsequent immunoblotting with pan-SOD1 pAbs. IP of wtSOD1 by DSE mAbs in G85R-transfected cells is consistent with similar misfolding induction or coincident IP of wtSOD1 with natively misfolded G85R protein (which possesses the DSE epitopes). Misfolded wtSOD1 was not detected in HEK cells transfected with the EV pFUW (Figs. 1*F* and 2*A*), so wtSOD1 misfolding was specifically induced by expression of the mutant SOD1 species and not due to cell stressors inherent in transfection.

The misfolded status of SOD1 isoforms in co-IP was also tested by digestion with protease K (PK; Fig. 2*B*). Natively

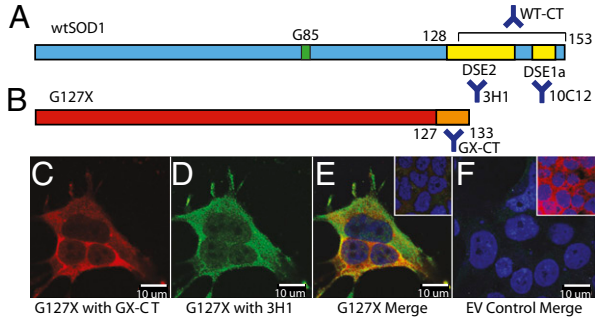

Fig. 1. Sequence overview of (*A*) wtSOD1 and (*B*) G127X SOD1. Residue G85 (mutated in some FALS cases) and the relative locations of the DSE, GX-CT, and WT-CT epitopes are noted, with the corresponding antibodies used in this study. The pan-SOD1 antibody used in this study was a rabbit polyconal antibody prepared by immunization with the whole wtSOD1 polypeptide. (*C–F*) Expression of G127X mutant misfolded SOD1 induces misfolding in wtSOD1. (*C* and *D*) IF images of G127X-transfected HEK 293FT (HEK) cells probed with (*C*) GX-CT polyclonal IgG, specific for the nonnative C terminus of G127X SOD1, and (*D*) the DSE2-specific mAb 3H1, which recognizes only misfolded full-length SOD1. (*E*) Merge of *C* and *D* with the nuclear-specific stain DAPI; *Inset:* untransfected cells stained with GX-CT, 3H1, and DAPI. Cells positive for 3H1 immunoreactivity also coexpress G127X. (*F*) Empty vector (EV) control stained with GX-CT, 3H1, and DAPI; *Inset:* EV control stained with DAPI and pan-SOD1 antibody.

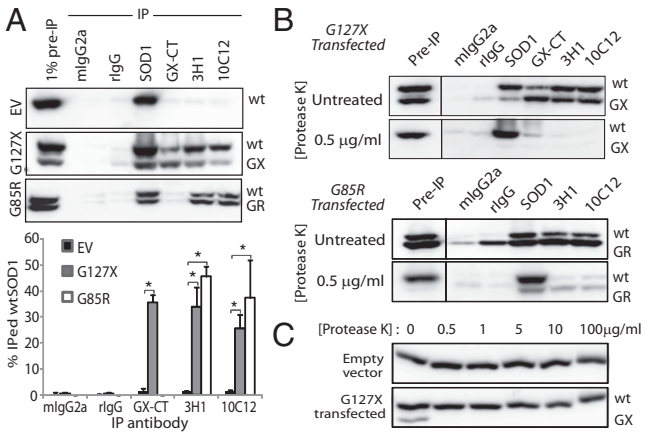

Fig. 2. Association with and conformational conversion of misfolded mutant SOD1 and misfolded wtSOD1. (*A*) IP of lysates from transiently transfected HEK cells. DSE mAbs 3H1 and 10C12 precipitate wtSOD1 in lysates from cells transfected with G127X or G85R but not with EV control. The quantitation summary is shown below; error bars represent SE. Values are the average of a minimum of five independent IP experiments. *Statistically significant difference compared with EV control. (*B*) IP of PK-treated lysates from G127X- and G85R-transfected HEK cells, demonstrating marked protease sensitivity exhibited by the mutant SOD1 variants and misfolded wtSOD1 immunoprecipitated by the DSE mAbs. A minimum of five replicates were performed for all immunoprecipitation experiments. (*C*) Protease sensitivity comparison of wtSOD1 and G127X mutant SOD1. Note that G127X is only detectable in the absence of PK. All immunoblots were probed with pan-SOD1 pAb.

structured wtSOD1 is highly resistant to PK, surviving exposure at concentrations up to 1.0 mg/mL (31), but G127X and G85R were sensitive to PK at low concentrations of <1.0 μg/mL (Fig. 2*B*). DSE mAb-immunoprecipitable wtSOD1 also displayed dramatic sensitivity to PK digestion at <1.0 μg/mL, consistent with enhanced PK access of the polypeptide backbone presumably due to structural loosening of the misfolded wtSOD1 isoform. The PK sensitivity of wtSOD1 in G85R transfection lysates confirmed that G85R induces misfolding of wtSOD1 and that co-IP is not merely due to physical association between natively folded wtSOD1 and G85R mutant protein. Thus, the presence of misfolded mutant SOD1 in the cytosolic compartment is associated with conformational conversion of human wtSOD1, as revealed by misfolding epitope exposure and marked protease sensitivity.

Mutant and wtSOD1 Form Nonnative Interchain Disulfide Linkages. In natively structured wtSOD1, monomers are stabilized by the Cys57–Cys146 intrachain disulfide bond. As Cys146 is deleted in G127X, Cys57 becomes available for nonnative disulfide linkages (24). In addition, Cys6, which is at the dimer interface of wtSOD1, is solvent-exposed in this natively monomeric mutant SOD1. Cys111 is also resident at the molecular surface. Our generation of specific complementary pAb probes for GX-CT and WT-CT afforded an opportunity to unambiguously determine the participation of G127X and wtSOD1 in multimers containing nonnative disulfide bonds. GX-CT direct immunoblots of G127X-transfected HEK cell lysates under nonreducing conditions revealed massive higher-order multimers of G127X and a minimal homodimer species band (≈33 kDa; Fig. S2, IV), all converting to monomer upon β-mercaptoethanol (β-ME) reduction (Fig. S2, II). These findings, which indicate that G127X can readily form nonnative interchain disulfide bonds, are in good agreement with analyzed CNS tissue from a G127X human patient (26) and G127X and L126Z transgenic mice (32, 33). Nonreducing immunoblots also revealed a ≈35-kDa band immunoreactive with GX-CT and WT-CT, which also converted to monomers upon reduction. This is consistent with a G127X-wtSOD1 heterodimer stabilized by nonnative interchain disulfide bonds. Only trace wtSOD1 is incorporated in G127X higher-order multimers, a finding confirmed by solubility experiments that show that G127X is the major SOD1 species present in detergent-resistant aggregates (Fig. S3*A*). Under nonreducing conditions the monomeric SOD1 band apparently migrated as a doublet, similar to previous studies (33), resolving to a single band with reduction and suggesting that wtSOD1 can also undergo intramolecular oxidative modifications.

Higher-order multimers and a prominent dimeric species at ≈34 kDa were also observed in G85R-transfected HEK cells, resolving to monomeric G85R and wtSOD1 in a reducing system (Fig. S2); the presence of WT-CT sequence in G85R obviated resolution of wtSOD1 in heterodimeric or multimeric species. Transfection of HEK cells with G127X SOD1 in which all Cys residues were mutated to Ser (designated "C-less G127X") revealed preserved conformational conversion of wtSOD1 (Fig. S3*B*), albeit at nonsignificantly lower levels than for Cys-containing G127X-transfected cells. Nonreducing immunoblots of lysates from these cells show C-less G127X almost exclusively in monomeric form, confirming that the 33-kDa, 35-kDa, and high molecular weight G127X-containing species are due to nonnative interchain disulfide linkages. We conclude that nonnative disulfide bonds are a consequence, and not a cause, of SOD1 misfolding, although they may stabilize misfolded species for co-IP.

W32 Is Involved in a Species-Specific Induction of wtSOD1 Misfolding by G127X SOD1. Motor neuron disease in mutant human SOD1 transgenic murine models of ALS can be accelerated by cross-breeding on transgenic mice expressing human wtSOD1, in which coaggregation of mutant and human wtSOD1 is observed (34–36). Endogenous murine SOD1 in these transgenic models seems to be essentially inert to aggregation (26, 36), although minor protective effects of mouse SOD1 have been observed (36). The epitopes for DSE1a and DSE2 are identical between mouse and human and can be exposed by oxidation-induced misfolding (Figs. S4*A* and S5). However, DSE immunoreactivity was not observed in transfected murine N2a neuroblastoma cells expressing abundant G127X protein (Fig. 3 *A* and *B*). Likewise, DSE mAb-immunoprecipitation was also not observed in lysates of N2a cells (Fig. S4*B*) compared with that of lysates from human HEK cells. Human restriction of G127X-induced wtSOD1 misfolding was confirmed in three human cell lines (HEK, HeLa, and SH-SY5Y) and three mouse cell lines (N2a, Min6, and B16; Fig. S4*B*). Notably, HEK and HeLa cells are mesenchymal, whereas SH-SY5Y cells are derived from a human neuroblastoma, suggesting that any cell type expressing human SOD1 is susceptible to mutant-induced misfolding.

Further inspection of the sequence revealed a strikingly nonconservative substitution of tryptophan (W) at position 32 in human SOD1 by serine in mouse SOD1. W32 is the only tryptophan in the human protein and has previously been identified as a site of oxidative modification and a potentiator of aggregation (37). Moreover, W32 is highly solvent exposed, ranking in the 89th percentile for solvent exposure among nonredundant tryptophans in the Protein Data Bank. G127X and G85R constructs with a W32S substitution had markedly reduced ability to convert wtSOD1 compared with these mutant proteins (Fig. 3 *C* and *D*), suggesting that W32 directly participates in the wtSOD1 conformational conversion process.

Misfolded wtSOD1 Is Sustained After Induction by Misfolding-Competent SOD1 Molecular Species. To understand whether induction of wtSOD1 misfolding was dependent on the continued

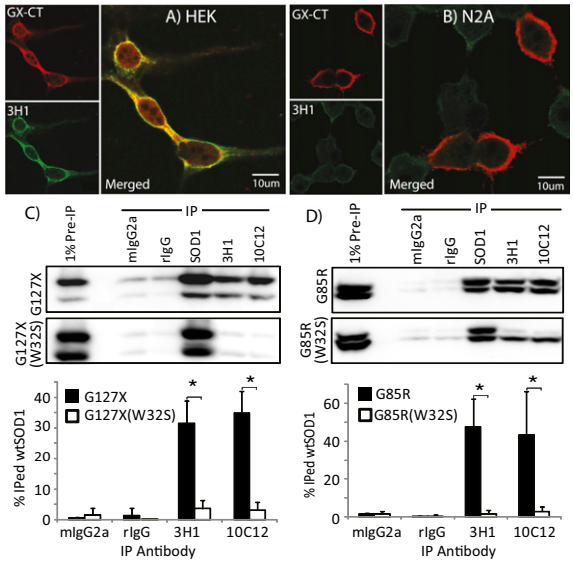

Fig. 3. Mouse SOD1 is not a substrate for conformational conversion by human misfolded SOD1, and a single missense mutation W32S in FALS-linked SOD1 mutants prevents conversion of wtSOD1 to a misfolded form. (*A* and *B*) IF images of G127X transiently transfected HEK (*A*) and mouse N2a (*B*) cells probed with GX-CT and 3H1 (the DSE2-specific mAb). HEK cells expressing G127X display 3H1 immunoreactvity for misfolded wtSOD1, but no 3H1 immunoreactivity is observed in N2a cells. (*C* and *D*) IP of lysates from HEK cells transfected with G127X/W32S (*C*) or G85R/W32S (*D*) double mutants. SOD1-DSE mAbs immunoprecipitate SOD1 from lysates endogenously expressing original FALS-linked SOD1 single mutants but not from those expressing the W32S mutation.

presence of mutant SOD1, HEK cells were transfected with G127X and monitored over time for levels of wtSOD1 misfolding. As a negative control, EV transfection and the extended duration of cell culture was not associated with any measurable wtSOD1 misfolding (Fig. S6). Maximal abundance of G127X protein was observed at 48 h, after which progressive depletion results in an undetectable level by day 6 (Fig. 4*A*). Transfection with G127X/W32S displayed a protein abundance time course similar to that of G127X (Fig. 4*B*). However, G127X expression induced wtSOD1 immunoreactivity with mAbs 3H1 and 12C12, which was detectable at day 2 and persisted to day 10, whereas expression of the G127X/W32S was not associated with detectable wtSOD1 misfolding at any point in the time course (Fig. 4 *A* and *B*), consistent with the W32-restricted wtSOD1 conformational conversion being directly mediated by the mutant species, and not due to nonspecific effects such as protein overexpression or chaperone titration. Moreover, the sustained high level of misfolded wtSOD1 at day 10 at least six half-lives (38) after peak G127X expression, and despite increased protease sensitivity of the misfolded species as determined in Fig. 2, suggests the possibility that misfolded wtSOD1 may propagate independently of mutant G127X. We further investigated this notion by overexpressing human wtSOD1, which has been noted in prior studies to be associated with a proportion of misfolded molecules (29, 30). In contrast to G127X, misfolded wtSOD1 possesses the C-terminal misfolding-specific epitopes recognized by 3H1 and 10C12, regardless of whether the protein originates from the transfection construct or endogenous wtSOD1 that has been induced to misfold. To effectively disentangle putative "converting" from "converted" species of wtSOD1, we compared time course concentrations of misfolded SOD1 in HEK cells transfected with wtSOD1 and wtSOD1/W32S constructs. Immunoreactivity with 3H1 and 10C12 peaked at 2 d for both constructs (Fig. 4*C*), as with G127X. However, at day 10 in the time course, wtSOD1/W32S-transfected cell lysates show a statistically significant decline in 3H1 and 10C12 immunoreactivity compared with wtSOD1 transfection ($P < 0.0001$; Fig. 4 *C* and *D*), consistent with the incompetence of the W32S species to induce a sustained wtSOD1 misfolding propagation.

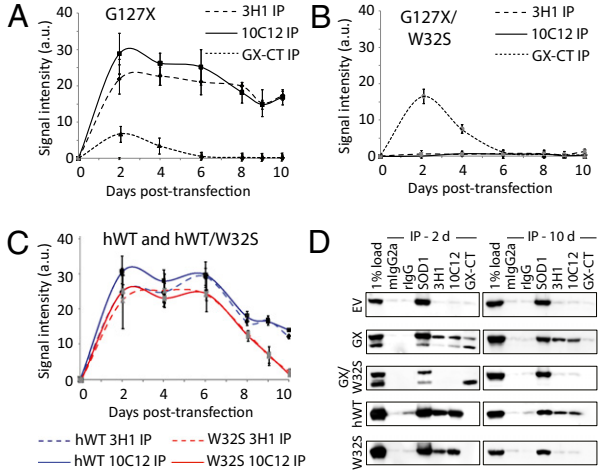

Fig. 4. Misfolded wtSOD1 is sustained after induction by misfolding-competent SOD1 molecular species. Lysates from cells collected at time points after transfection were examined by immunoprecipitation with DSE mAbs 3H1 and 10C12, and the relative amount of immunoprecipitated misfolded SOD1 calculated and represented in graphical form over time. (*A*) G127X vs. (*B*) G127X/W32S; G127X/W32S is incompetent to induce wtSOD1 misfolding, but G127X-induced wtSOD1 misfolding persists at least 4 d after G127X is no longer detectable, consistent with wtSOD1 misfold propagation. The relative abundance of the expressed transgene (in G127X in *A* and G127X/W32S in *B*) is shown by GX-CT IP. (*C*) Overexpressed hWT SOD1 vs. overexpressed W32S SOD1. No antibody probes exist to distinguish whether misfolded SOD1 derives from transfection or endogenous SOD1. There is a significant difference at day 10 of DSE immunoreactivity for wtSOD1 vs. SOD1/W32S transfectants ($P < 0.0001$, Mann-Whitney test). (*D*) Representative immunoblots (probed with pan-SOD1 pAb) from HEK cell lysates collected 2 d and 10 d after transfection with EV, G127X, G127X/W32S, hWT SOD1, and W32S SOD1.

G127X Induces wtSOD1 Misfolding in a Recombinant Cell-Free System. Induced misfolding of wtSOD1 prompted us to investigate the role of the intracellular milieu in the process, including non-SOD1 macromolecules. Purified recombinant wtSOD1 (Fig. S7) was incubated with and without preaggregated recombinant G127X for 24 h with agitation at 37 °C in Hepes-buffered saline in the presence or absence of DTT (50 mM) and EDTA (5 mM) to simulate the reducing and extensively metal cation-buffered intracellular environment. Misfolded wtSOD1 was measured in a Biacore surface plasmon resonance assay by capture with 3H1 mAb. G127X significantly potentiated wtSOD1 misfolding in the solution containing DTT and EDTA (Fig. 5*A*), although a limited background of spontaneous misfolding of wtSOD1 was observed under these conditions. Conversely, in the solution without DTT or EDTA, there was no induction of wtSOD1 misfolding either in the presence or absence of G127X (Fig. 5*B*). The misfolded SOD1 generated in the cell-free system was sensitive to degradation by PK (Fig. 5*D*), as also observed for

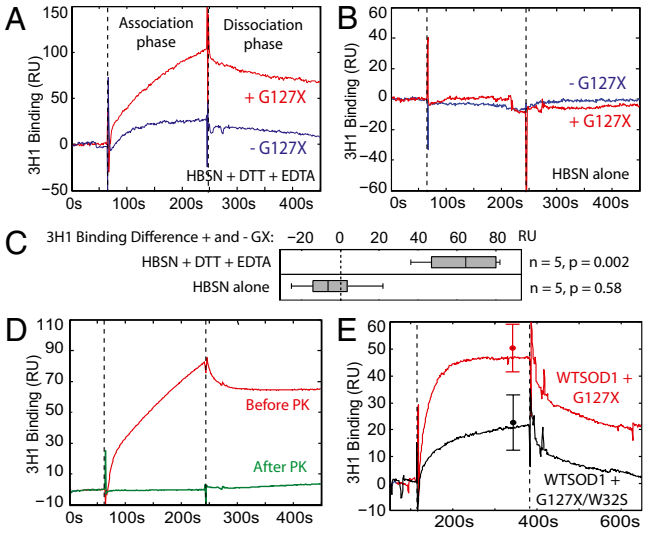

Fig. 5. Recombinant G127X can induce wtSOD1 misfolding in a cell-free system under reducing, metal cation-buffered conditions. (*A*) Representative Biacore sensorgram showing misfolded SOD1 binding to 3H1 mAb after 24 h incubation at 37 °C in the presence and absence of recombinant misfolded G127X protein in Hepes-buffered saline (HBSN) containing 50 mM DTT and 5 mM EDTA. Analyte is applied to the sensor surface during the association phase and allowed to elute during the dissociation phase. (*B*) Same experiment as in *A* performed in Hepes buffered saline without DTT or EDTA. (*C*) Box plot showing difference in 3H1 binding between 24-h incubated samples in the presence and absence of G127X for both buffer conditions. Binding levels are normalized to account for variation in immobilization levels of 3H1 between replicates. In the buffer containing DTT and EDTA there is a significant increase in 3H1 binding when G127X is added (99% confidence interval 22–103 response units, RU), whereas in the buffer without DTT or EDTA there is no significant difference due to the addition of G127X (95% confidence interval −26 to 17 RU). *P* values reported are from a paired *t* test of independent replicates. (*D*) Treatment of misfolded wtSOD1 generated by coincubation with G127X with PK (1 μg/mL for 30 min) causes its complete degradation. (*E*) Coincubation with G127X/W32S causes significantly less induction of wtSOD1 misfolding compared with coincubation with G127X ($P = 0.02$). Error bars show mean and SD of binding at the end of the association phase for three independent experimental replicates.

misfolded wtSOD1 in cell culture (Fig. 2*B*). Coincubation with purified G127X/W32S instead of G127X induced considerably less wtSOD1 misfolding (Fig. 5*E*), confirming the protective effect of the W32S substitution. These results suggest that wtSOD1 as a metal replete dimer can still intermittently expose its intrachain disulfide bond for reduction and "trapping" in a partially misfolded state recognized by the 3H1 electrostatic loop mAb, and also indicates that natively misfolded G127X protein can facilitate this process. Reduction of the monomer disulfide bond has been previously shown to precipitate further structural disorganization in wtSOD1 and increase its propensity for aggregation (24). Moreover, no other macromolecule seems to be essential for the SOD1 conformational conversion reaction, consistent with direct physical interaction between isoforms. Although the solution conditions used in these experiments approximate the reducing and metal cation-buffered intracellular milieu, we cannot be sure that they recapitulate the cytosolic environment exactly.

Discussion

We have developed tractable reductionist systems in vitro using SOD1 isoform-specific antibodies to dissect the molecular mechanisms of mutant-induced wtSOD1 misfolding. We demonstrate unambiguously that cytosolic expression of misfolded SOD1 mutants G127X and G85R can confer a misfolded conformation on wtSOD1, as revealed by exposure of natively inaccessible peptide epitopes and markedly enhanced protease sensitivity consistent with structural loosening.

Conformational conversion of wtSOD1 by copper-deficient G127X and G85R SOD1 mutants is accompanied by formation of nonnative SOD1 interchain disulfide bonds and C-terminal oxidation at C146, both indicative of a prooxidant environment. Previous studies have recognized SOD1 nonnative disulfide bond formation but have posited that this reaction takes place in the oxidizing environment of mitochondria (34). Indeed, mutant misfolded SOD1 has been found to be associated with the outer membrane of mitochondria purified from SOD1 mutant transgenic mouse spinal cords (22), of which a proportion is lodged in the voltage-dependent anion channel-1 (39). However, we report a diffuse cytosolic immunoreactivity for G127X and misfolded wtSOD1 in transfected HEK cells, suggesting that mitochondria are not the only cellular compartment in which SOD1 can become oxidized and cross-linked. Previous studies demonstrate that disulfide-bonded SOD1 multimers are dependent on the availability of convertible wtSOD1 (34), which supports the notion that misfolded wtSOD1 is the source of oxidative species, at least transiently.

Our systems have enabled us to determine that conformational conversion of human wtSOD1 is sequence-restricted, dominated surprisingly by a single residue: W32. This residue is substantially solvent-exposed on the external convexity of the protein, distant from the native dimer interface. The implication of this "alternate site" for SOD1-SOD1 interaction may resolve some seeming conflicts related to the participation of wtSOD1 in transgenic mouse models of ALS. In transgenic mice expressing human SOD1 mutants, the presence or absence of murine endogenous SOD1 has minimal impact on clinical disease, and murine SOD1 is not incorporated in mutant human SOD1 aggregates (34–36). Mouse SOD1 possesses a Ser residue at position 32, which we now report is unable to participate in misfolding reactions with human wtSOD1 through this site, although dimer interface interactions are not precluded (40, 41). By contrast, human wtSOD1 expression can dramatically accelerate clinical disease in transgenic mice expressing a range of human SOD1 mutants and is associated with incorporation of human wtSOD1 in aggregates (34–36, 41). Human SOD1 possesses the W32 residue, which we report in this article is essential for misfolding induction of wtSOD1 in HEK cells. However, some studies have shown that human wtSOD1 can actually stabilize mutant SOD1, thought to be due to the formation of native heterodimers mediated by the dimer interface (41–43). It has also been noted (41, 43) that coaggregation of mutant and wtSOD1 is not a simple stoichiometric process, confirmed by our study: massive W32-dependent disulfide-stabilized multimers are observed for G127X and G85R, but incorporation of wtSOD1 in these multimers is minimal, retaining solubility in nondenaturing detergents, consistent with our detected monomer and/or nonnative disulfide-bonded heterodimers. The role of W32 in the mutant misfolded inducing species is also supported by a recent study showing that wild-type human SOD1 does not accelerate motor neuron disease in mice expressing murine SOD1 with the G86R mutation (44), which lacks a W32 residue.

The conformational conversion of natively structured SOD1 is analogous to the conversion of the natively folded prion protein (PrP^{C}) to a misfolded conformer of the same protein (PrP^{Sc}) in prion disease. Two mechanisms have been proposed to account for the $PrP^{C}\rightarrow PrP^{Sc}$ conversion process: nucleation–polymerization, in which the misfolded monomeric PrP^{Sc} is intrinsically less stable as a monomer but becomes more stable than PrP^{C} when recruited to a multimolecular PrP^{Sc} aggregate; and template mediated assistance, in which the PrP^{Sc} conformer is more stable than PrP^{C} but kinetically inaccessible without catalysis by interaction with PrP^{Sc} (15). Seeded polymerization of proteins can be regarded as recruitment of partially unfolded molecular species to an aggregate, whereas in template assistance, partially unfolded recruitable intermediates are first generated by contact between natively folded molecular species and the template. Future study is needed to understand how the SOD1 misfolding mechanism can be placed in this conceptual framework, but one may speculate from the evidence above that the misfolding mechanisms of mutant SOD1 and wtSOD1 span a continuum from seeded polymerization to template assistance. Aggregation of partially unfolded mutant SOD1 may propagate primarily by seeded polymerization, whereas conversion of wtSOD1 may necessitate structural loosening induced by contact with a mutant or even wild-type misfolded template (45) before recruitment to the misfolded SOD1 seed. In support of this notion is the recent finding that wtSOD1 can only participate in seeded polymerization on exposure to low pH and the chaotrope guanidine in vitro (12, 46), conditions that destabilize the native state and favor seeded polymerization.

Overexpression of wtSOD1 in the present study (Figs. S2 and S4) and in other laboratories (29, 30) is associated with induction of misfolding in a proportion of SOD1 molecules. Recent studies have shown misfolded wtSOD1 in sporadic as well as SOD1 FALS (12, 13, 47), suggesting that the stochastic generation of misfolded SOD1 template might trigger sporadic ALS, as has been theorized for sporadic prion disease. However, a recent study (14, 48) using different antibodies than the above (12, 13) identified SOD1 aggregates from SOD1 FALS but not sporadic ALS patients. These data are consistent with different SOD1 misfolding epitope exposure in SOD1 FALS and typical SALS and perhaps even different mechanisms for SOD1 aggregation, as suggested above. Demonstration of prion-like intercellular mutant SOD1 aggregate propagation (20) therefore contributes to understanding of the FALS disease process, but its relevance to SALS is obscure. The present study shows a clear role for intracellular induction of wtSOD1 misfolding either by wtSOD1 overexpression or mutant SOD1 transfection, moving a step closer to a unified model of FALS and SALS pathogenesis.

Materials and Methods

Refer to *SI Materials and Methods* for details.

Immunoprecipitation. Refer to *SI Materials and Methods* for detailed methods. Briefly, transfected cells were lysed, and 100 μL of cell lysate was mixed with 10 μL of antibody-coupled M-280 Tosyl-activated magnetic Dynabeads, then in-

cubated for 3 h at room temperature with constant rotation. Beads were washed three times and boiled in SDS sample buffer containing 1% β-mercaptoethanol for 5 min. One microliter of lysate was added directly into SDS sample buffer, boiled, and used as a pre-IP control. The generation of mouse monoclonal DSE antibodies used in IP experiments is described elsewhere (21, 22).

Protease Analyses of Misfolded SOD1. HEK cells were transiently transfected with G127X- or G85R-SOD1 for 48 h. Cells were lysed without protease inhibitors, and 400-μL aliquots from each lysate were digested with a concentration series of proteinase K for 30 min at 37 °C. Digests were terminated by the addition of protease inhibitor mixture and phenylmethylsulfonyl fluoride to a final concentration of 5 mM.

Statistical Analyses. At least five independent experiments were subjected to statistical analysis. The nonparametric Mann-Whitney test was used to determine differences between IP experiment quantitation in Figs. 2*A* and 5 and Figs. S2 and S3, comparing the pairs of independent samples. In experiments involving multiple groups (more than two cell lines, species, groupings, etc., in Figs. 4*B* and 6) the nonparametric Kruskal-Wallis test was used. The Bonferroni correction was applied to multiple comparisons; significance was set at $P < 0.05$ in all cases and indicated by asterisks (*). Statistical analyses were performed using SPSS 17.0 and XLSTAT 2008.

ACKNOWLEDGMENTS. We thank Trent Bjorndahl, T. Dean Airey, and Rose Lee for technical assistance and Amorfix Life Sciences and Biogen-Idec for access to the disease-specific epitope mAbs. Biacore experiments were performed in the Michael Smith Biothermodynamics Laboratory, University of British Columbia. N.R.C. is the Canada Research Chair in Neurodegeneration and Protein Misfolding Diseases at the University of British Columbia and is supported by donations from the Allen T. Lambert Neural Research Fund and the Temerty Family Foundation, as well as by grants from PrioNet Canada and the Canadian Institutes of Health Research (CIHR). S.S.P. is supported by grants from the Natural Sciences and Engineering Research Council and the A. P. Sloan Foundation. W.C.G. received a Vanier Canada Graduate Scholarship from CIHR.

1. Cleveland DW, Rothstein JD (2001) From Charcot to Lou Gehrig: Deciphering selective motor neuron death in ALS. *Nat Rev Neurosci* 2:806–819.
2. Rowland LP, Shneider NA (2001) Amyotrophic lateral sclerosis. *N Engl J Med* 344: 1688–1700.
3. Haverkamp LJ, Appel V, Appel SH (1995) Natural history of amyotrophic lateral sclerosis in a database population. Validation of a scoring system and a model for survival prediction. *Brain* 118:707–719.
4. Rosen DR, et al. (1993) Mutations in Cu/Zn superoxide dismutase gene are associated with familial amyotrophic lateral sclerosis. *Nature* 362:59–62.
5. Andersen PM (2000) Genetic factors in the early diagnosis of ALS. *Amyotroph Lateral Scler Other Motor Neuron Disord* 1(Suppl 1):S31–S42.
6. Gurney ME, et al. (1994) Motor neuron degeneration in mice that express a human Cu,Zn superoxide dismutase mutation. *Science* 264:1772–1775.
7. Ilieva H, Polymenidou M, Cleveland DW (2009) Non-cell autonomous toxicity in neurodegenerative disorders: ALS and beyond. *J Cell Biol* 187:761–772.
8. Hart PJ (2006) Pathogenic superoxide dismutase structure, folding, aggregation and turnover. *Curr Opin Chem Biol* 10:131–138.
9. Kato S, et al. (2000) New consensus research on neuropathological aspects of familial amyotrophic lateral sclerosis with superoxide dismutase 1 (SOD1) gene mutations: Inclusions containing SOD1 in neurons and astrocytes. *Amyotroph Lateral Scler Other Motor Neuron Disord* 1:163–184.
10. Bruijn LI, et al. (1997) ALS-linked SOD1 mutant G85R mediates damage to astrocytes and promotes rapidly progressive disease with SOD1-containing inclusions. *Neuron* 18:327–338.
11. Durham HD, Roy J, Dong L, Figlewicz DA (1997) Aggregation of mutant Cu/Zn superoxide dismutase proteins in a culture model of ALS. *J Neuropathol Exp Neurol* 56: 523–530.
12. Bosco DA, et al. (2010) Wild-type and mutant SOD1 share an aberrant conformation and a common pathogenic pathway in ALS. *Nat Neurosci* 13:1396–1403.
13. Forsberg K, et al. (2010) Novel antibodies reveal inclusions containing non-native SOD1 in sporadic ALS patients. *PLoS ONE* 5:e11552.
14. Kerman A, et al. (2010) Amyotrophic lateral sclerosis is a non-amyloid disease in which extensive misfolding of SOD1 is unique to the familial form. *Acta Neuropathol* 119: 335–344.
15. Horwich AL, Weissman JS (1997) Deadly conformations—protein misfolding in prion disease. *Cell* 89:499–510.
16. Aguzzi A (2009) Cell biology: Beyond the prion principle. *Nature* 459:924–925.
17. Ravits JM, La Spada AR (2009) ALS motor phenotype heterogeneity, focality, and spread: Deconstructing motor neuron degeneration. *Neurology* 73:805–811.
18. Urushitani M, et al. (2006) Chromogranin-mediated secretion of mutant superoxide dismutase proteins linked to amyotrophic lateral sclerosis. *Nat Neurosci* 9:108–118.
19. Meissner F, Molawi K, Zychlinsky A (2010) Mutant superoxide dismutase 1-induced IL-1beta accelerates ALS pathogenesis. *Proc Natl Acad Sci USA* 107:13046–13050.
20. Münch C, O'Brien J, Bertolotti A (2011) Prion-like propagation of mutant superoxide dismutase-1 misfolding in neuronal cells. *Proc Natl Acad Sci USA* 108:3548–3553.
21. Cashman N, et al. (2007) Active and passive immunization of superoxide dismutase-1 disease-specific epitopes in a mouse model of amyotrophic lateral sclerosis. *Ann Neurol* 62:542–543.
22. Vande Velde C, Miller TM, Cashman NR, Cleveland DW (2008) Selective association of misfolded ALS-linked mutant SOD1 with the cytoplasmic face of mitochondria. *Proc Natl Acad Sci USA* 105:4022–4027.
23. Rakhit R, et al. (2007) An immunological epitope selective for pathological monomer-misfolded SOD1 in ALS. *Nat Med* 13:754–759.
24. Tiwari A, Xu Z, Hayward LJ (2005) Aberrantly increased hydrophobicity shared by mutants of Cu,Zn-superoxide dismutase in familial amyotrophic lateral sclerosis. *J Biol Chem* 280:29771–29779.
25. Elam JS, et al. (2003) Amyloid-like filaments and water-filled nanotubes formed by SOD1 mutant proteins linked to familial ALS. *Nat Struct Biol* 10:461–467.
26. Jonsson PA, et al. (2004) Minute quantities of misfolded mutant superoxide dismutase-1 cause amyotrophic lateral sclerosis. *Brain* 127:73–88.
27. Cao X, et al. (2008) Structures of the G85R variant of SOD1 in familial amyotrophic lateral sclerosis. *J Biol Chem* 283:16169–16177.
28. Rodriguez JA, et al. (2002) Familial amyotrophic lateral sclerosis-associated mutations decrease the thermal stability of distinctly metallated species of human copper/zinc superoxide dismutase. *J Biol Chem* 277:15932–15937.
29. Jaarsma D, et al. (2000) Human Cu/Zn superoxide dismutase (SOD1) overexpression in mice causes mitochondrial vacuolization, axonal degeneration, and premature motoneuron death and accelerates motoneuron disease in mice expressing a familial amyotrophic lateral sclerosis mutant SOD1. *Neurobiol Dis* 7(6 Pt B):623–643.
30. Cozzolino M, et al. (2008) Cysteine 111 affects aggregation and cytotoxicity of mutant Cu,Zn-superoxide dismutase associated with familial amyotrophic lateral sclerosis. *J Biol Chem* 283:866–874.
31. Ratovitski T, et al. (1999) Variation in the biochemical/biophysical properties of mutant superoxide dismutase 1 enzymes and the rate of disease progression in familial amyotrophic lateral sclerosis kindreds. *Hum Mol Genet* 8:1451–1460.
32. Zetterström P, et al. (2007) Soluble misfolded subfractions of mutant superoxide dismutase-1s are enriched in spinal cords throughout life in murine ALS models. *Proc Natl Acad Sci USA* 104:14157–14162.
33. Furukawa Y, Fu R, Deng HX, Siddique T, O'Halloran TV (2006) Disulfide cross-linked protein represents a significant fraction of ALS-associated Cu, Zn-superoxide dismutase aggregates in spinal cords of model mice. *Proc Natl Acad Sci USA* 103: 7148–7153.
34. Deng HX, et al. (2006) Conversion to the amyotrophic lateral sclerosis phenotype is associated with intermolecular linked insoluble aggregates of SOD1 in mitochondria. *Proc Natl Acad Sci USA* 103:7142–7147.
35. Wang L, et al. (2009) Wild-type SOD1 overexpression accelerates disease onset of a G85R SOD1 mouse. *Hum Mol Genet* 18:1642–1651.
36. Bruijn LI, et al. (1998) Aggregation and motor neuron toxicity of an ALS-linked SOD1 mutant independent from wild-type SOD1. *Science* 281:1851–1854.
37. Taylor DM, et al. (2007) Tryptophan 32 potentiates aggregation and cytotoxicity of a copper/zinc superoxide dismutase mutant associated with familial amyotrophic lateral sclerosis. *J Biol Chem* 282:16329–16335.
38. Borchelt DR, et al. (1994) Superoxide dismutase 1 with mutations linked to familial amyotrophic lateral sclerosis possesses significant activity. *Proc Natl Acad Sci USA* 91: 8292–8296.
39. Israelson A, et al. (2010) Misfolded mutant SOD1 directly inhibits VDAC1 conductance in a mouse model of inherited ALS. *Neuron* 67:575–587.
40. Borchelt DR, et al. (1995) Superoxide dismutase 1 subunits with mutations linked to familial amyotrophic lateral sclerosis do not affect wild-type subunit function. *J Biol Chem* 270:3234–3238.
41. Witan H, et al. (2009) Wild-type Cu/Zn superoxide dismutase (SOD1) does not facilitate, but impedes the formation of protein aggregates of amyotrophic lateral sclerosis causing mutant SOD1. *Neurobiol Dis* 36:331–342.
42. Roberts BR, et al. (2007) Structural characterization of zinc-deficient human superoxide dismutase and implications for ALS. *J Mol Biol* 373:877–890.
43. Prudencio M, Durazo A, Whitelegge JP, Borchelt DR (2010) An examination of wild-type SOD1 in modulating the toxicity and aggregation of ALS-associated mutant SOD1. *Hum Mol Genet* 19:4774–4789.
44. Audet JN, Gowing G, Julien JP (2010) Wild-type human SOD1 overexpression does not accelerate motor neuron disease in mice expressing murine Sod1 G86R. *Neurobiol Dis* 40:245–250.
45. Rakhit R, et al. (2004) Monomeric Cu,Zn-superoxide dismutase is a common misfolding intermediate in the oxidation models of sporadic and familial amyotrophic lateral sclerosis. *J Biol Chem* 279:15499–15504.
46. Chia R, et al. (2010) Superoxide dismutase 1 and tgSOD1 mouse spinal cord seed fibrils, suggesting a propagative cell death mechanism in amyotrophic lateral sclerosis. *PLoS ONE* 5:e10627.
47. Cashman NR, Griffin JK, Sehgal S (2002) Allele-selective recruitment and disease progression in familial amyotrophic lateral sclerosis. *Neurology* 58:A79.
48. Liu HN, et al. (2009) Lack of evidence of monomer/misfolded superoxide dismutase-1 in sporadic amyotrophic lateral sclerosis. *Ann Neurol* 66:75–80.

Supporting Information

Grad et al. 10.1073/pnas.1102645108

SI Materials and Methods

Immunoprecipitation. Transfected cells growing on 100-mm dishes were washed twice in ice-cold PBS and collected by centrifugation (5 min at 1,000 × *g*, 4 °C). Cell pellets were lysed in 400 μL lysis buffer [PBS, 0.5% sodium deoxycholate (DOC), 0.5% Triton X-100, and 1× complete, EDTA-free protease inhibitor mixture; Roche Diagnostics] for 2 min on ice, followed by centrifugation for 5 min at 1,000 × *g*, 4 °C. Lysate was removed to a fresh tube. For immunoprecipitation (IP) experiments, 100 μL cell lysate was added to 0.6-mL microfuge tubes. Ten microliters of antibody-coupled M-280 Tosyl-activated magnetic Dynabeads (Dynal Biotech) were added to each tube and mixed. Tubes were incubated for 3 h at room temperature with constant rotation. Beads were then washed three times with 150 μL RIPA buffer [150 mM NaCl, 50 mM Tris-HCl (pH 8.0), 1% Nonidet P-40, 0.5% DOC, and 0.1% SDS] with brief vortexing between washes, and boiled in SDS sample buffer containing 1% β-mercaptoethanol for 5 min. One microliter of lysate was added directly into SDS sample buffer, boiled, and used as a pre-IP control.

DNA Mutagenesis and Cloning. SOD1 cDNA was subcloned into the expression vector pFUW (1), and all subsequent mutagenesis was performed on this template using the PCR. For amplification of the human wild-type SOD1 (wtSOD1) and G127X, the forward primer used was 5′-CCGTCTAGAGGATCCACCACCATGGCGACGAAGGCC-3′. The reverse primer for hWT and A4V SOD1 was 5′-CGGAATTCTAGATTATTGGGCGATCCCAATTACACC-3′; for G127X, 5′-CCGGAATTCCTATTTCCATCGTTGGCCGCCCAAGTCATCTGCTTTTTCATGGACCACC-3′. For amplification of the A4V mutation, the forward primer was 5′-GTTAGACAGGATCCCGACACCACCATGGCGACGAAGGTCGTGTGCGTGCTGAAG-3′. For amplification of G85R mutation, the primers used were 5′-GTTGGAGACTTGCGCAATGTGACTGCTG-3′ and 5′-CAGCAGTCACATTGCGCAAGTCTCCAACATG-3′. For amplification of the G127Xm24-36 mutation, the primers used were 5′-GCAAGCGGTGAACCAGTTGTGTTGTCAGGACAAATTACAGGACTGACTGAAGG-3′ and 5′-TGTAATTTGTCCTGACAACACAACTGGTTCACCGCTTGCCTTCTGCTCGAAATTG-3′. For cysteine-less G127X, each of the three cysteine residues were systematically mutated to serine, and mutagenized PCR products were subcloned back into pFUW-G127X to provide a template for further cysteine substitutions. For the C6S substitution, the primers used were 5′-CGCGGATCCCGACACCACCATGGCGACGAAGGCCGTGTCAGTGCTGAAGG-3′ and 5′-CGGAATTCTAGATTATTGGGCGATCCCAATTACACC-3′. For the C57S substitution, the primers used were 5′-GGAGATAATACAGCAGGCTCAACCAGTGCAGGTCCTCAC-3′ and 5′-GTGAGGACCTGCACTGGTTGAGCCTGCTGTATTATCTCC-3′. For the C111S substitution, the primers used were 5′-CTCTCAGGAGACCATTCAATCATTGGCC-3′ and 5′-GGCCAATGATTGAATGGTCTCCTGAGAG-3′. The mutated PCR products were extracted from agarose gels using an extraction kit (Invitrogen), digested with BamH1 and EcoR1 restriction enzymes, and recloned into pFUW-SOD1 or pFUW-G127X where appropriate. All mutated constructs were sequence-confirmed.

Cell Culture and Transfection. All reagents for cell cultures were purchased from Invitrogen. The cell lines used for this study were all cultured in DMEM supplemented with 10% FBS, 10 U/mL penicillin, 10 μg/mL streptomycin, and 2 mM L-glutamine. Cells were transiently transfected with Lipofectamine LTX (Invitrogen) as indicated by the manufacturer. Forty-eight hours after transfection, cells were processed as described for each experiment.

Molecular Dynamics Simulation of Wild-Type and G127X SOD1. All-atom molecular dynamics was performed using NAMD (2) with the CHARMM22 force field, a time step of 2 fs, particle-mesh Ewald electrostatics, periodic boundary conditions, and a Lennard-Jones cutoff distance of 13.5 Å. Proteins were solvated in a box of explicit water molecules that exceeded the dimensions of the native protein by 10 Å on all sides. Basic residues (Lys and Arg) were protonated, acidic residues (Asp and Glu) were deprotonated, and histidines were neutrally charged to reflect ionization conditions at pH 7. Na^+ and Cl^- ions were added to the solvent to achieve overall system charge neutrality and an ionic strength of 150 mM. For wtSOD1, the simulation was run for a total of 20 ns, and data from the last 18 ns of the simulation were used to calculate residue root mean square deviation. For G127X, the crystal structure of wtSOD1 with residues 134–153 removed, and residues 127–133 mutated from the wild-type sequence to the G127X sequence, was used as a starting point for simulation. This structure was first equilibrated and minimized with a 20-ns simulation to arrive at a candidate structure for G127X; the result of this simulation was used as a starting point for a second 20-ns simulation, from which residue root mean square deviation values for G127X were calculated. Calculation of stability difference between wtSOD1 and S32W mutant mouse SOD1 was performed with the ERIS analysis tool (3).

Preparation of Antibody-Coupled Magnetic Dynabeads. Beads (175 μL) were washed twice in 1 mL PBS and resuspended in a final volume of 1 mL PBS. Eighty micrograms of disease-specific epitope (DSE) monoclonal antibody, 50 μg pan-SOD1 (SOD100; Assay Designs), or 125 μL GX-CT polyclonal antibodies were added to beads and incubated for 24 h at 37 °C with constant rotation (100 μg BSA, mouse IgG2a, or rabbit IgG were coupled to beads as negative controls). Beads were then washed twice in 1 mL PBS, 0.1% BSA, and incubated in 1 mL blocking buffer [0.2 M Tris-HCl (pH 8.5) and 0.1% PBS] for 4 h at 37 °C with constant rotation. Beads were then washed twice in 1 mL PBS, 0.1% BSA, resuspended in a final volume of 500 μL of PBS, and stored at 4 °C.

Immunofluorescence Microscopy. HEK 293FT or N2a cells were placed on glass coverslips in a 24-well plate 1 d before transfection. Cells were transfected for 48 h with Lipofectamine LTX (Invitrogen) according to the manufacturer's protocol and processed for the immunofluorescence assay as follows. Cells were washed three times with ice-cold PBS (pH 7.4) and fixed in 4% paraformaldehyde (in PBS) for 15 min at room temperature. Fixed cells were then washed/permeabilized three times for 5 min in PBS-T (0.3% Triton-X-100 in PBS) and incubated with 10 μg/mL GX-CT or pan-SOD1 pAb, or 2 μg/mL 3H1 mAb, diluted in PBS-T with 2% normal goat serum, for 1 h at room temperature. Cells were then washed three times in PBS-T and incubated with appropriate secondary antibody conjugated to Alexa Fluor 488 (green) or Alexa Fluor 647 (red) dyes [Invitrogen (Molecular Probes)] for 1 h at room temperature in the dark. For DNA staining, DAPI stain was used (300 nM in PBS). DAPI-stained cells were incubated for 10–15 min at room temperature after a first wash of secondary antibody, followed by three more washes with PBS. Cells were mounted with a glass

coverslip in a drop of Fluoromount-G (SouthernBiotech) and allowed to dry overnight before imaging. Images were viewed and captured on an Olympus FluoView FV1000 microscope (Olympus Canada).

SDS/PAGE and Immunoblotting. Boiled samples were either analyzed on 15% or 4–20% acrylamide Tris-Glycine gels, as indicated. For nonreduced samples, cell lysates of equal endogenous SOD1 concentrations were prepared with 100 mM iodoacetamide (Acros Organics), a nonreversible sulfhydryl-blocking agent, and boiled in SDS sample buffer in the absence of the reducing agent β-mercaptoethanol. Proteins were electrophoretically transferred to PVDF membrane, blocked with 5% milk in Tris-buffered saline, 0.1% Tween-20 (TBS-T) for 1 h, and incubated with SOD100 antibody in 5% milk–TBS-T for 1 h at room temperature or overnight at 4 °C with constant rocking. Membranes were washed with TBS-T followed by 1-h incubation with donkey anti-rabbit IgG, horseradish peroxidase-linked whole antibody (GE Healthcare) diluted 1:5,000 in 5% milk–TBS-T. Membranes were then developed with ECL-Plus chemiluminescent substrate (GE Healthcare) and visualized using a VersaDoc Imager (Bio-Rad Laboratories), and signal intensities were quantified using Quantity One software (Bio-Rad Laboratories). Final values of immunoprecipitable material are the mean average of four or more independent experiments and expressed as a percentage of the total immunoprecipitable SOD1 (the amount of SOD1 immunoprecipitated by pan-SOD1 pAb). WT-CT and GX-CT polyclonal rabbit antibodies were raised against peptides corresponding to either the carboxyl-terminal end of wtSOD1 (amino acids 128–153) or against the distinct carboxyl-terminal of G127X-SOD1 (GGQRWK); these were generated and purified by GenScript. Both antibodies were used at 5 μg/mL for immunoblotting. For the detection of protein carbonyls, cell lysates of equal protein concentration were treated using the OxyBlot Kit (Millipore) according to the manufacturer's instructions, separated by SDS/PAGE, and immunoblotted as above using the polyclonal anti-DNP provided. Total protein from cell lysates was determined using the bicinchoninic acid assay kit (Sigma). Quantitation of total carbonyl signal for each lane was performed as above; DNP signal quantitation was normalized to β-tubulin (monoclonal; Sigma-Aldrich). Values represent the average of six independent experiments.

Time Course Experiment. HEK cells were transfected as described above with the constructs indicated in Fig. 5 (main text) [one of empty vector (EV), G127X, G127X/W32S, WTSOD1, or W32S SOD1] and at 2, 4, 6, 8, 9, and 10 d after transfection for IP and Western blot with pan-SOD1 antibody. Media was changed on the cells every 2 d after transfection. All experiments were repeated in triplicate.

Differential Detergent Extraction. SOD1 aggregation was determined by differential detergent extraction as described in ref. 4, with modifications. Specifically, HEK cells grown on 60-mm tissue culture dishes were transiently transfected with the indicated construct for 48 h. Cells were washed twice in ice-cold PBS, collected by centrifugation (5 min at 1,000 × *g*, 4 °C), and the pellets were resuspended in 100 μL TNE buffer [10 mM Tris-HCl (pH 8), 1 mM EDTA (pH 8), and 100 mM NaCl]. Cell suspensions were mixed with an equal volume of 2× extraction buffer (TNE supplemented with 1% Nonidet P-40 and 2× protease inhibitor mixture), homogenized using 25-gauge needles attached to 1-mL syringes, and centrifuged for 5 min at 1,000 × *g*, 4 °C. Lysates were collected in 1.5-mL microfuge tubes and centrifuged for 8 min at 100,000 × *g* in a TLA100.3 rotor to separate the supernatant (S1) from the pellet (P1). The P1 pellet was washed once with PBS and resuspended in 200 μL of 1× extraction buffer (TNE, 0.5% Nonidet P-40, and 1× protease inhibitor mixture) using 25-gauge needles. The extracts were then centrifuged for 8 min at 100,000 × *g* in a TLA100.3 rotor (Beckman) to obtain the nonionic detergent-insoluble pellet (P2). The P2 pellet was resuspended in 90 μL of 1× extraction buffer and subjected to trichloroacetic acid precipitation before being resuspended in 1× SDS sample buffer and subjected to SDS/PAGE and immunoblotting.

Recombinant SOD1 Production and Purification. The gene for human wtSOD1 was purchased from DNA2.0. All reagents were purchased from Sigma and Fisher, except for the nickel-NTA, resin which was purchased from Qiagen. The gene encoding human wtSOD1 was inserted into a pET15b vector between the NcoI and EcoRI restriction sites. The mutant G127X SOD1 gene was created by standard PCR methods using oligonucleotides that inserted NcoI and EcoRI sites at the initiation codon and after the stop codon. The digested and purified gene fragment, corresponding to G127X SOD1, was introduced into a pET15b vector. The identity of the mutation and the correctness of gene insertion (location and orientation) were verified by DNA sequencing. Both proteins were expressed in *Escherichia coli* BL21(DE3) host cells in LB medium supplemented with 100 μg/mL ampicillin. The cultures were grown at 37 °C until an OD_{600} = 0.8 was reached and then induced with 1.0 mM IPTG for 18 h at 25 °C. $CuSO_4$ (3 mM) and $ZnSO_4$ (30 μM) were also added at the time of isopropyl-β-D-thiogalactopyranoside (IPTG) induction. After induction the cells were harvested by centrifugation (9,060 × *g* for 20 min).

The cells were lysed on ice by sonication in lysis buffer (25 mM Tris, 25 mM NaCl, and 1 EDTA-free protease inhibitor mini-tablet per 10 mL, pH 8.0). The wtSOD1 protein was then isolated and purified from the lysate via one-step ion metal affinity chromatography using a Ni-NTA column. More specifically, the cell lysate containing the wtSOD1 was centrifuged at 48,400 × *g* for 1 h (25 °C) to remove cellular debris and the supernatant loaded onto a Ni-NTA column (10-mL bed volume) preequilibrated with lysis buffer (25 mM Tris and 25 mM NaCl, pH 8.0). The column was then washed with several wash buffers [buffer 1: 25 mM Tris, 25 mM NaCl (pH 8.0), 0.2% Triton X-100; buffer 2: 50 mM Tris, 50 mM NaCl, 10 mM $MgSO_4$, 1 mM $MgCl_2$, and 1 mM $CaCl_2$, pH 7.5] and eluted with an imidazole elution buffer (50 mM Tris, 50 mM NaCl, 10 mM $MgSO_4$, 1 mM $MgCl_2$, 1 mM $CaCl_2$, and 600 mM imidazole, pH 7.5). The wtSOD1 protein was then concentrated to 10 mg/mL using an Amicon Ultra-15 centrifugal device with imidazole removal and buffer exchange into 25 mM KH_2PO_4/K_2HPO_4 and 25 mM NaCl, pH 7.0. Metallation of purified wtSOD1 was confirmed by inductively coupled plasma mass spectrometry (ICP-MS), run on an ELAN 6000 ICP-MS analyzer. The ratio of protein to metals was found to be Protein:Cu:Zn = 2.1 mg/mL: 8.2 ppm: 9.9 ppm = 130 μM: 129 μM: 152 μM = 1:1:1.16. The slight stoichiometric excess of zinc is believed to be due to residual binding to the His tag on the protein.

The mutant G127X SOD1 was purified from the inclusion bodies under denaturing conditions on an Ni-NTA column. Specifically, the inclusion bodies were solubilized with an inclusion body solubilization buffer (25 mM Tris, 25 mM NaCl, and 8 M Urea, pH 8.0) and then incubated overnight at room temperature in the same buffer followed by centrifugation at 48,000 × *g* for 1 h at 25 °C. The cleared protein solution was loaded onto an Ni-NTA column (10 mL bed volume) preequilibrated with the inclusion body solubilization buffer. The mutant G127X SOD1 was then eluted from the Ni-NTA column after series of the washing steps using identical washing and elution buffers as above, except with the addition of 6 M urea. Preparation of G127X/W32S proceeded equivalently.

In Vitro G127X-Mediated Misfolding Induction of Recombinant wtSOD1 Protein. Before use, the stock solution of G127X or G127X/W32S was buffer exchanged into 10 mM Hepes-buffered 150 mM NaCl with two washings by centrifugation at 5,000 × *g* in an Amicon 3-kDa cutoff 15-mL cellulose filter tube (Millipore) to a concentration of 0.16 mg/mL.

For the in vitro conversion assay, incubation buffer was prepared containing 10 mM Hepes-buffered 150 mM NaCl (HBSN), pH 7.4 as a base. DTT and EDTA were added to the HBSN to a final concentration of 50 mM DTT plus 5 mM EDTA for the experiments in Fig. 5 *A*–*C* (main text), and 10 mM DTT plus 5 mM EDTA for the experiments in Fig. 5 *D* and *E* (main text). Samples were prepared in incubation buffer containing 100 μg/mL wtSOD1 plus 10 μg/mL G127X or G127X/W32S; the total volume of each sample was 120 μL. Samples were incubated in sealed tubes at 37 °C with rotation for 24 h for experiments shown in Fig. 5 *A*–*C* (main text) and 48 h for experiments in Fig. 5 *D* and *E* (main text). For the protease sensitivity experiment in Fig. 5*D* (main text), protease K at a final concentration of 1 μg/mL was added to the samples after incubation and left at 37 °C for 30 min before adding protease inhibitor mixture and phenylmethylsulfonylfluoride to a final concentration of 5 mM.

Measurement of misfolded wtSOD1 was performed using a BiaCore 3000 surface plasmon resonance detector (GE Healthcare). Surfaces 1 and 2 of a CM5 sensor chip were activated by a 1:1 mixture of ethyl(dimethylaminopropyl) carbodiimide (EDC) and *N*-hydroxysuccinimide (NHS), 3H1 mAb was applied only to surface 2, aiming for an immobilization level of 10,000 response units, then ethanolamine was applied to both surfaces to block remaining immobilization sites. Thus, surface 2 was used as the active surface with immobilized 3H1 antibody, whereas surface 1 was used as a reference surface that was activated and blocked without antibody immobilization. The signal on reference surface 1 was subtracted from the signal on active surface 2 in all sensorgrams used for data analysis. HBSN buffer (10 mM Hepes and 150 mM NaCl, pH 7.4) was used as the running buffer in the BiaCore instrument.

Samples were injected into flow cells 1 and 2 at 20 μL/min for 3 min during an association phase (5 min in Fig. 5*E*, main text), followed by a 3-min dissociation phase during which running buffer passed through the flow cells at 20 μL/min. Between samples, the sensor chip surface was regenerated to remove any adherent SOD1 protein by washing with pH 2.0 10 mM glycine HCl buffer for 45 s at a flow rate of 30 μL/min. Sensorgrams were linearly detrended to remove baseline drift when present. Differences in 3H1 binding between samples with and without added G127X from each experiment replicate were calculated and examined for significance using a paired *t* test. Sensorgram analysis was performed with BiaEvaluation software (GE Healthcare).

1. Lois C, Hong EJ, Pease SS, Brown EJ, Baltimore D (2002) Germline transmission and tissue-specific expression of transgenes delivered by lentiviral vectors. *Science* 295: 868–871.
2. Phillips JC, et al. (2005) Scalable molecular dynamics with NAMD. *J Comput Chem* 26: 1781–1802.
3. Yin S, Ding F, Dokholyan NV (2007) Eris: An automated estimator of protein stability. *Nat Methods* 4:466–467.
4. Karch CM, Borchelt DR (2008) A limited role for disulfide cross-linking in the aggregation of mutant SOD1 linked to familial amyotrophic lateral sclerosis. *J Biol Chem* 283:13528–13537.

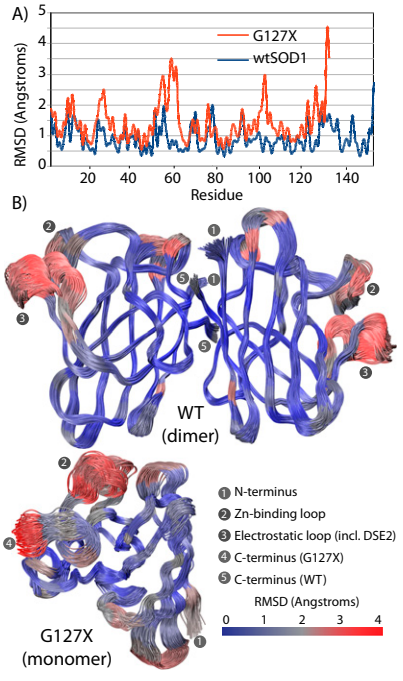

Fig. S1. G127X SOD1 mutant protein displays structural instability. (*A*) Comparison of residue-by-residue root mean square deviations between wtSOD1 and G127X from 20-ns all-atom molecular dynamics. (*B*) One hundred superimposed protein conformers of wt and G127X SOD1 taken from molecular dynamics simulation and shaded according to the root mean square deviation of backbone C-α atoms. Interestingly, the greatest regional fluctuations in molecular dynamics simulation of wtSOD1 are seen in the vicinity of the electrostatic loop containing DSE2 and near DSE1a, which suggests that these epitopes are present in relatively unstable parts of the protein that are most susceptible to immunologically detectable conformational changes.

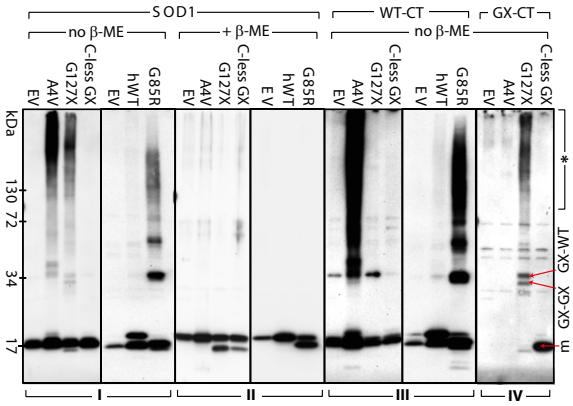

Fig. S2. G127X forms nonnative disulfide interactions with wtSOD1. Lysates from HEK cells transiently transfected with different SOD1 variants were separated on 4–20% acrylamide gels by SDS/PAGE, either in the absence (I, III, and IV) or presence (II) of the reducing agent β-mercaptoethanol (β-ME) and probed with either pan-SOD1, GX-CT, or WT-CT pAbs. m, monomer; GX-GX, G127X homodimer; GX-WT, G127X-wtSOD1 heterodimer; C-less, cysteine-less version of G127X. *High molecular weight species. A minimum of four independent replicates were performed for each antibody and reducing condition. An apparent dimer of wtSOD1 is observed in the EV transfection developed by WT-CT antibodies, which may represent native dimers surviving SDS/PAGE or disulfide-linked nonnative dimers due to oxidative cell stress of transfection.

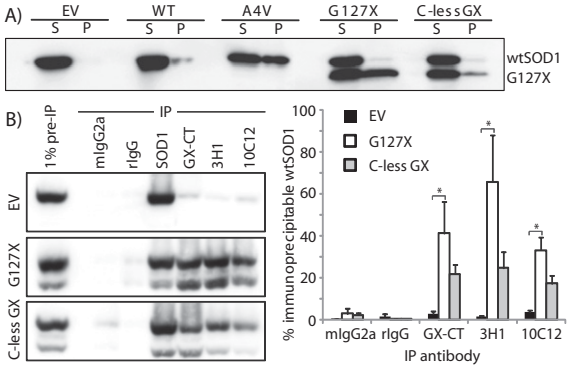

Fig. S3. Cysteine nonnative disulfide bonds are dispensable in SOD1 conformational conversion. (*A*) Lysates from HEK cells transiently transfected with different SOD1 constructs were solubilized with nondenaturing detergent and subjected to differential centrifugation to generate a detergent-soluble (S) fraction and a highly detergent-insoluble pellet (P). Fractions were separated by SDS/PAGE and probed with pan-wtSOD1 antibody. Four independent replicates were performed for each transfectant. (*B*) IP of lysates from HEK cells transfected with EV, G127X, or a cysteine-less version of G127X (C-less GX). Immunoblots were probed with pan-SOD1 pAb. The absence of cysteines in G127X does not prevent conversion of wtSOD1, although a nonsignificant decrease in efficiency is observed. Quantitation summary is included; values represent the average of at least five independent replicates per transfectant, and error bars represent SE. *Statistically significant difference compared with EV control.

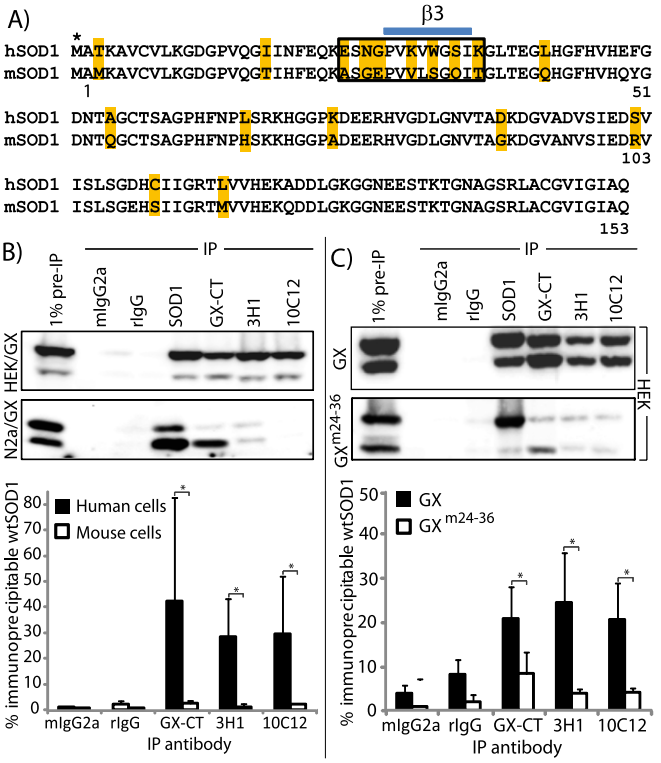

Fig. S4. Mutant SOD1-mediated wtSOD1 misfolding is sequence/structure-specific. (*A*) Sequence alignment of human SOD1 (hSOD1) and mouse SOD1 (mSOD1) proteins. Orange blocks indicate nonconserved residues. Box indicates region of chimeric substitution enriched in human–mouse differences. Location of the SOD1 divergence motif (loop II and β-strand 3) is indicated by blue line. *Initial methionine cleaved during processing. Human and mouse SOD1 are highly conserved, sharing 83% sequence identity (BLAST) and 89% sequence similarity (T-COFFEE sequence alignment). However, visual inspection of the sequence in *A* reveals a divergent region comprising loop II and β-strand 3 of the SOD1 β-barrel (codons 24–36), in which 7 of the 13 residues are non-homologous. We therefore tested whether the determinants for wtSOD1 conversion might map to this nonconserved region by swapping mouse amino acid sequence 24–36 into human G127X and transfecting this construct (G127X^{m24-36}) into HEK cells. (*B*) IP of lysates from HEK or N2a cells transfected with G127X. DSE mAbs 3H1 and 10C12 precipitate wtSOD1 in lysates from human HEK cells but not from mouse N2a cells. The quantitation summary below includes data from three human (HEK, SH-SY5Y, and HeLa) and three mouse (N2a B16, and MIN6) cell lines. (*C*) IP of HEK cells transfected with human G127X or the human–mouse G127X^{m24-36} chimera. DSE mAbs precipitate misfolded wtSOD1 in G127X-transfected cells but not in G127X^{m24-36}-transfected cells. For all immunoprecipitation experiments, a minimum of four independent replicates were performed for each cell line and construct. All immunoblots in *B* and *C* were probed with pan-SOD1 pAb. Error bars in quantitation summaries represent SE. *Significant difference between two indicated measurements. Pre-IP levels of the G127X construct were 47.2 ± 4.5 signal volume (arbitrary units), whereas pre-IP levels of G127X^{m24-36} were 52.8 ± 4.5 (a nonsignificant difference). Although G127X^{m24-36} was expressed at similar levels to the parent G127X construct, conversion of human wtSOD1 was ablated. These data indicate that the hSOD1 24–36 residue domain is required for efficient recruitment of wtSOD1 by G127X, consistent with structural or sequence dependence for conformational conversion of wtSOD1.

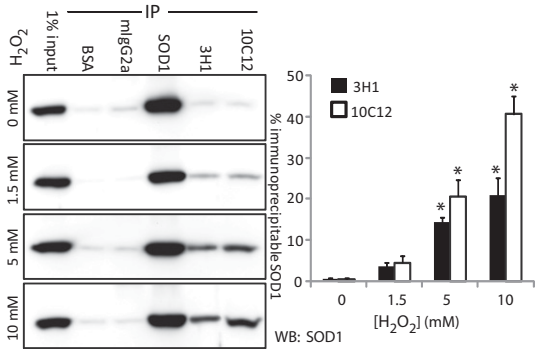

Fig. S5. SOD1-DSE mAbs can detect endogenous misfolded SOD1 in mouse cells. IP of lysates from mouse N2a cells pretreated with different concentrations of hydrogen peroxide for 45 min at 37 °C. SOD1-DSE mAbs immunoprecipitate endogenous mouse SOD1 in lysates from cells exposed to an oxidative insult but do not immunoreact with SOD1 from untreated cells. Immunoblots probed with pan-SOD1 pAb. Values in quantitation are corrected for nonspecific immunereactivity, and summaries represent average of three independent experiments. Error bars represent SD. *$P < 0.05$ compared with untreated control, using unpaired *t* test.

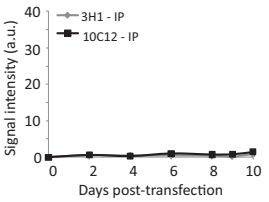

Fig. S6. Additional data for the time course experiment shown in Fig. 4 (main text). Transfection with an empty vector construct did not cause detectable wtSOD1 misfolding during the time course experiment.

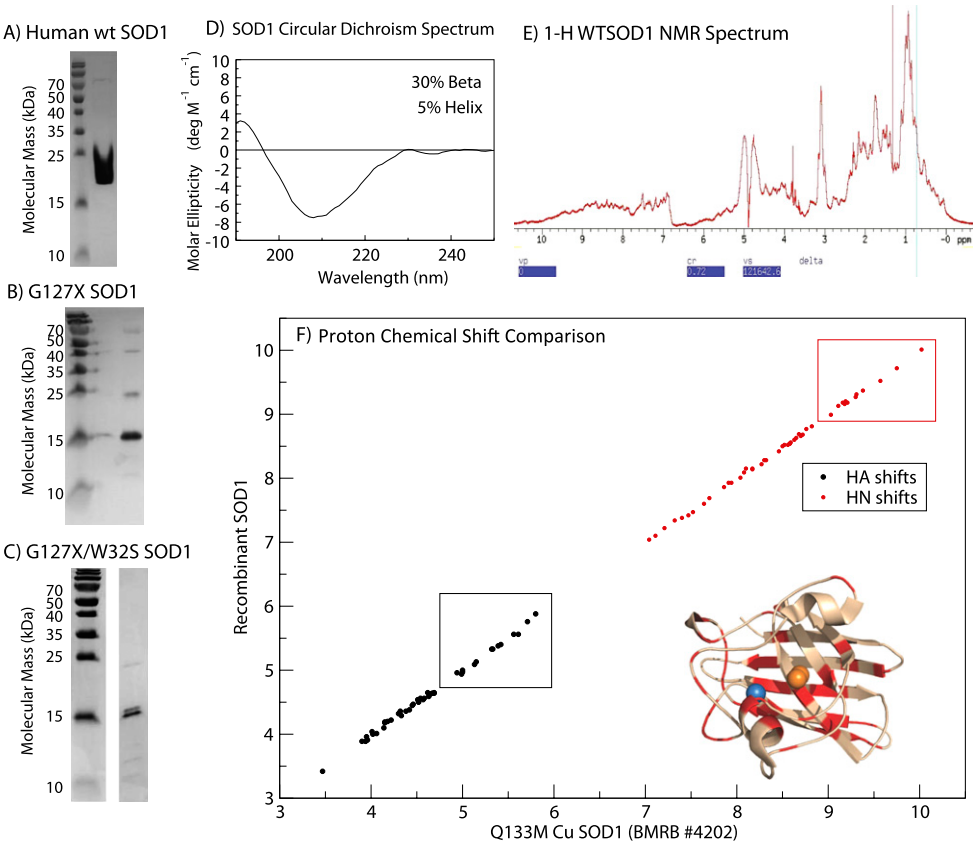

Fig. S7. Purification of recombinant SOD1. (*A*) A 15% SDS/PAGE gel of human wtSOD1 purified from *E. coli* in 25 mM KH_2PO_4/K_2HPO_4 buffer. (*B*) A 15% SDS/PAGE gel of human G127X SOD1 purified from *E. coli* in 6 M urea, 25 mM Tris, 25 mM NaCl, 1 mM $CaCl_2$, 10 mM $MgSO_4$, 1 mM $MgCl_2$, and 600 mM imidazole at pH 7.3. (*C*) A 15% SDS/PAGE gel of human G127X/W32S SOD1 purified from *E. coli* in 6 M urea, 25 mM Tris, 25 mM NaCl, 1 mM $CaCl_2$, 10 mM $MgSO_4$, 1 mM $MgCl_2$, and 600 mM imidazole at pH 7.3. (*D*) Circular dichroism (CD) spectrum of folded wtSOD1. The sample was 1 mg/mL in the same buffer described in *A*. The CD was collected on an OLIS-17 spectrophotometer. Five scans were averaged between 190 and 260 nm with 1-nm increments. The resulting spectra were averaged and smoothed over a 5-nm window. The percentage of secondary structure was calculated using CDPro from the SPX22 subset and the ContinLL program. The resulting secondary structure was 4.4% helix and 29.9% sheet, which is in strong agreement with the Protein Data Bank deposited structure 2V0A (33% β and 6% helix). (*E*) A 1-H NMR spectrum of dimeric recombinant human wtSOD1, demonstrating that it has correctly folded as indicated by the well-dispersed amide signals (6–10 ppm) and the strong, dispersed α 1-H signal (4.5–6.0 ppm). These indicate the presence of high levels of β-sheet (α 1-H signals) and stable tertiary structure (the amide 1-H signals). (*F*) Correspondence of amide proton (HN) chemical shifts (black) and alpha proton (HA) shifts assigned by proton TOCSY (red) between NMR measurements of recombinant protein prepared for the cell-free conversion assay and previously deposited assignments for SOD1. Chemical shifts for residues colored red in the *Inset* SOD1 structure were used. Boxes are placed around the downfield HN and HA chemical shifts; these downfield shifts are consistent with β structure and support the CD spectra in *D*. This comparison with published chemical shifts for metallated SOD1 shows a high degree of correlation and is evidence that the protein is correctly folded.